Effect of cylinder wall parameters on the final packing density of mono-disperse spheres subject to three-dimensional vibrations

Grogan, Jack R.; Nicuşan, Andrei L.; Windows-Yule, Christopher R.K.

DOI:
10.1016/j.partic.2024.01.017

Document Version
Publisher's PDF, also known as Version of record

Citation for published version (Harvard):
Grogan, JR, Nicuşan, AL & Windows-Yule, CRK 2024, 'Effect of cylinder wall parameters on the final packing density of mono-disperse spheres subject to three-dimensional vibrations', *Particuology*, vol. 91, pp. 211-225. https://doi.org/10.1016/j.partic.2024.01.017

Particuology 91 (2024) 211–225

Contents lists available at ScienceDirect

Particuology

journal homepage: www.elsevier.com/locate/partic

Effect of cylinder wall parameters on the final packing density of mono-disperse spheres subject to three-dimensional vibrations

Jack R. Grogan, Andrei L. Nicuşan, Christopher R.K. Windows-Yule*

School of Chemical Engineering, The University of Birmingham, Edgbaston, Birmingham, B15 2TT, UK

ARTICLE INFO

Article history:
Received 6 October 2023
Received in revised form
14 January 2024
Accepted 29 January 2024
Available online 8 February 2024

Keywords:
Vibropacking
Packing
Densification
Vibration
Discrete element method
Friction
Wall friction
Restitution

ABSTRACT

Achieving densely packed particles is desirable within the industries of ceramics, pharmaceuticals, defence and additive manufacturing. In this work, we use the discrete element method (DEM) to determine the effect of wall parameters on the final packing density of mono-disperse spheres subject to 4 varying three-dimensional vibration and fill conditions. We focus specifically on the impact of the container wall parameters on the particles' final packing density. Following on from the validation of the DEM simulation the particle-wall coefficient of restitution, the particle-wall coefficient of rolling friction and the particle-wall coefficient of sliding friction were varied individually and the effect on the final packing density analysed. For relatively low particle-particle friction glass beads, the effect of these wall properties had no discernible effect on the final packing density achieved. Following on from these findings the particle-wall properties were varied at the extreme values of particle-particle coefficient of rolling friction and particle-particle coefficient of sliding friction. For a particle-particle coefficient of sliding friction = 1, increases in particle-wall coefficient of restitution resulted in a minor increase in the final packing density of particles though this was not statistically significant. For a particle-particle coefficient of sliding friction = 1, increases in particle-wall coefficient of rolling friction resulted in a minor decrease in the final packing density of the particles though again not to a degree where the trend can, with complete certainty, be distinguished from the random error across the repeats. Finally, when the particle-particle coefficient of sliding friction = 1, increases in particle-wall coefficient of sliding friction resulted in a significant decrease in the final packing density of particles. This decrease was attributed to the propagation of force chains throughout the packing. The significant decrease in final packing density with particle-wall coefficient of sliding friction highlights the need to choose appropriate vessel materials to optimise packing of particles with a high particle-particle coefficient sliding friction. Conversely, for particles with minimal particle-particle friction, the particle-wall friction coefficient has no effect on the final packing density of particles - a potentially valuable finding for certain industrial applications. All simulations were run using the open-source DEM package LIGGGHTS on the University of Birmingham's high-performance computer: BlueBEAR. All the code files used within this paper can be found on Github: https://github.com/Jack-Grogan/DEM-Vibropacking-Wall-Effects.

1. Introduction

1.1. Background

The issue of generating a very dense packing of particles has a wide range of applications in the industries of ceramics (White & Walton, 1937; Ayer & Soppet, 1965), pharmaceuticals (Salamat et al., 2022), defence and additive manufacturing (Zhou et al., 2009; Salamat et al., 2022). Particle packing is also of significant importance in the loading of packed towers throughout the industry (Ayer & Soppet, 1965). Due to high particle packing densities being desirable in many industries, a large body of research has looked into optimising packing density. A common technique used throughout the industry is densification through vibration (Hettiarachchi & Mampearachchi, 2018). A lot of work to date has focused on optimising vibration parameters to various particle geometries. An overview of current work in the field can be found in the literature review below. The focus of this study is to determine the effect to which the properties of the container the particles are packed in, influences the final packing density of particles

* Corresponding author.
E-mail address: c.r.windows-yule@bham.ac.uk (C.R.K. Windows-Yule).

https://doi.org/10.1016/j.partic.2024.01.017

following three-dimensional vibration. An understanding of the effect of wall properties on final packing density will give industry an idea of the implications of changing from 3D printed or perspex designs, to aluminium or steel during scale-up; knowledge valuable to ensuring test systems can accurately model real systems.

1.2. Literature review

Early work in the field was performed in 1944 by Oman and Watson (1944) (Zhang, 2004). Oman and Watson coined the terms "random dense" and "random loose" to respectively describe the maximal and minimal densities of randomly packed mono-sized spheres (Zhang, 2004). In the 1960s further developments were made in the field with the aim of quantifying the maximum packing density for a range of scenarios. Scott's work in 1960 focused on the arrangement of uniform mono-sized spheres in random loose and random dense packing arrangements (Scott, 1960). Scott found that 1/8 inch diameter steel balls in a range of vessel geometries (cylinders and spheres), when extrapolated to an infinite size, hence removing wall effects, had a packing density of approximately 0.63(7) for dense packing and 0.60(1) for loose packing (Scott, 1960). It is worth noting that the maximal packing density obtained in these early experiments for mono-sized spheres, 0.63(7) (Scott, 1960), is considerably lower than the packing densities achieved later on when the packing method and vibration were optimised, 0.7399 (Li et al., 2011). The Kepler conjecture states that the maximum attainable packing density of spheres occurs when spheres form a face-centred cubic arrangement with a density of $\pi/\sqrt{18} \approx 0.74048$ (Hales, 2005). In 1969 Scott and Kilgour improved on Scott's 1960 findings by adding an extra magnitude of precision to Scott's values for maximum packing density (Scott & Kilgour, 1969). In 1961 McGeary utilised mechanical vibration to generate densely packed binary, ternary and quaternary systems of spheres in square and cylindrical containers. McGeary found that an optimal packing density was achieved when each sphere size differed by a factor of 7 (McGeary, 1961). This optimal was attributed to the triangular pore size of the spheres (McGeary, 1961). McGeary was able to generate a packing density at 95.1% of the theoretical density for a quaternary packing of spheres with diameter ratios 1:7:38:316; the theoretical maximum packing density for these particle sizes was calculated as 0.975 (McGeary, 1961). J. E. Ayer and F. E. Soppet in addition to McGeary showed that ordering of particles by the walls for steel shot in steel cylinders and metal shot in glass cylinders, respectively, can be neglected when the ratio between sphere diameter and cylinder diameter (d/D ratio) is less than 0.1 (Ayer & Soppet, 1965; McGeary, 1961; Hettiarachchi & Mampearachchi, 2018). However, work conducted by Yu and An et al. found that the wall properties can still influence the dynamics of a system at wall diameter ratios lower than this finding a significant increase in packing density as d/D ratio decreased from 0.08 to 0.02 (Yu et al., 2006). The effect of the walls on bulk system behaviour is discussed further by Windows-Yule et al. (2013) (Windows-Yule et al., 2018). Further information about the early work in the field can be found in the work of Zhang (2004) and Hettiarachchi and Mampearachchi (2018) with more recent work in the field discussed in the introduction of Salamat et al. (2022).

Following on from this early work into packing densities, computer simulation along with experimental research has been employed to determine the packing densities of a range of mono-sized regular shapes: simulation work with spherical particles (An et al., 2008; Yu et al., 2006; An et al., 2005; Zhang et al., 2001), experimental work with spherical particles (Li et al., 2011; An & Li, 2013; An et al., 2009; Reimann et al., 2017); simulation work with cubic particles (Wu et al., 2017), experimental work with cubic particles (Xie et al., 2017); simulation work with tetrahedral particles (Zhao et al., 2017), simulation and experimental work with tetrahedral particles (Zhao, An, Wang, et al., 2020); simulation work with cylindrical particles (Qian et al., 2018), experimental work with cylindrical particles (Qian et al., 2016); experimental work with ellipsoid particles (Li, Zou, et al., 2020); simulation and experimental work with octahedral particles (Wang et al., 2021); and experimental work with dodecahedral particles (Li, An, et al., 2020) to reference a few. Work by Roskilly et al. (2010) also explored the behaviour of different combinations of aspherical particles (including rods, cubes, and plate-like particles) finding a complex interplay between packing density and segregation (Rosato & Windows-Yule, 2020). Work conducted by Wu et al. extrapolated maximum packing densities as high as 0.727 following vibration of cubic particles in simulation (Wu et al., 2017). Experimental work on the packing of cubes conducted by Xie et al. achieved packing densities of 0.844 (Xie et al., 2017). Zhoa et al. were able to achieve packing densities of 0.7402 for simulation of regular tetrahedral particles when extrapolated to remove wall effects (Zhao et al., 2017). Simulation work for packing of cylinders conducted by Qian et al. found packing density following vibration and extrapolation to be 0.7166 (Qian et al., 2018). Physical studies of cylinder packing conducted Qian et al. with differing vibration conditions and cylinder geometry were able to achieve packing densities of 0.73 following extrapolation (Qian et al., 2016). Experimental work on ellipsoid packing conducted by Li et al. was able to achieve packing densities as high as 0.76 though also found that packing density is highly dependent on the aspect ratio of the ellipsoids (Li, Zou, et al., 2020). Experimental work conducted by Li et al. with dodecahedral particles was able to achieve packing densities of 0.709 when extrapolated to remove the influence of container walls (Li, An, et al., 2020).

The effect of vibration has also been studied extensively. Work conducted by An et al. on mono-sized spheres under one-dimensional (An et al., 2009) and two-dimensional vibration (An & Li, 2013) and C. X. Li and An et al.'s work on three-dimensional vibrations (Li et al., 2011), attained packing densities of 0.636, 0.6757 and 0.6890 respectively for the "total feeding method" and packing densities of 0.663, 0.7131 and 0.7399 respectively for the "batch feeding method". For the total feeding method, all the particles were added at once prior to vibration, for the batch feeding method an optimum number of particle layers were added at regular time intervals during vibration. An et al. found the increase in final packing density from reducing batch size plateaued once the batch size decreased below one particle layer; batch size was therefore set as 1 particle layer for the batch filling packing density results (An et al., 2009; An & Li, 2013; Li et al., 2011). Work conducted by Windows-Yule et al. showed that manipulation of the vibration amplitude during the densification process can significantly alter the final packing density of particles compared to equivalent systems vibrated at constant amplitude, allowing in some cases for higher packing densities to be achieved (Windows-Yule, Rosato, et al., 2014; Windows-Yule, Weinhart, et al., 2014). Following on from the work on mono-sized systems under vibrations some research has also been conducted into the packing densities of binary systems under vibration (An et al., 2016; Hettiarachchi & Mampearachchi, 2018; An & Chai, 2016) and systems of multiple geometrically dissimilar regular shapes under vibration (An et al., 2015; Zhao, An, Zhao, et al., 2020). Continuous-size distributions have been found to pack differently for mono-sized and binary systems (Yu & Standish, 1993). Little research so far has been conducted on the packing behaviour of continuous-size distributions of particles under vibration. A paper by Salamat et al. (Salamat et al., 2022) investigated the formation of dense

packing of a continuous-size distribution of spherical particles under one-dimensional vibrations through the use of DEM and found that local density values become “quite uniform” at optimal vibration parameters (Salamat et al., 2022). Research conducted by Yang et al. investigated both simulation and physical experimentation of three-dimensional vibration of Gaussian particle distributions (Yang et al., 2020). Yang found that vibration intensity did not directly relate to particle packing density, but however, highlighted that for each vibration frequency, there exists an optimal amplitude to generate a dense packing. Yang's experimental results for 300 μm particles with a standard deviation of 0.2 generated packing densities as high as 0.84 (Yang et al., 2020). Yang found higher vibration frequencies to generate denser packing with optimal packing amplitude decreasing with an increase in frequency (Yang et al., 2020). Almost all research to date has modelled particles settling in containers of cylindrical or cuboid geometry with some of the very early work being conducted in spherical containers. Research as of yet has not looked to model irregular shapes that would be more representative of the particles used in industry, it would also be interesting to know how irregularly shaped spheres affect the optimal particle size ratio of 7 calculated for quaternary systems of spheres (McGeary, 1961). Finally, research into the effect of material properties on final packing density has to date only concerned the particle-particle properties, no research exists on the effect of the particle-wall properties on the final packing density. These areas provide a good focus for future research, the focus of this paper is to determine the effect of particle-wall properties on the final packing density.

1.3. Focus of current study

Research undertaken by An et al. found that an increase in particle-particle coefficient of sliding friction significantly reduced the final packing density, whereas an increase in particle-particle coefficient of rolling friction only slightly reduced the final packing density (An et al., 2008). The effect of particle-particle coefficient of restitution was investigated by Zhang et al. (Zhang et al., 2001). Zhang et al. found that the final packing density of particles increased with increasing coefficient of restitution when poured into a container (Zhang et al., 2001). To date, all research around the friction and restitution coefficients has concerned the particle-particle interactions. The focus of this study is to assess to what degree the particle-wall coefficients of friction and restitution affect the final packing density. The paper begins by validating the DEM model against Yu et al.'s and An et al.'s simulations of vibrating glass beads. An and Yu are leaders in the field of DEM, with work that has been validated against data from physical experiments (An et al., 2008; Yu et al., 2006; Yu, 2004). The paper goes on to study the effect of the particle-wall coefficient of restitution, coefficient of rolling friction and coefficient of sliding friction on the final packing density of glass beads. Finally, the paper looks into the effect of these three wall properties at the extremes of particle-particle friction.

2. Methods

2.1. Introduction to DEM

To address the focus of this study the discrete element method (DEM) simulations were implemented using the open-source DEM package LIGGGHTS. LIGGGHTS allows for simulation of vibration of the container base and walls to impart energy to the particles. All simulations were run on the University of Birmingham's high-performance computer: BlueBEAR (University of Birmingham, 2023). All the code files used within this paper can be found on Github: https://github.com/Jack-Grogan/DEM-Vibropacking-Wall-Effects. DEM models, unlike experimental methods, provide full information regarding the dynamics and mechanics of particulate systems. However, without precise calibration, DEM models can be highly inaccurate (Windows-Yule et al., 2016; Windows-Yule & Neveu, 2022). To ensure the validity of our results, our simulations have been calibrated against prior data (see section 3.1). A comprehensive discussion of the validity of DEM can be found in the work of C. R. K. Windows-Yule et al. (Windows-Yule et al., 2016).

2.2. Simulation setup

The simulation was validated through quantitative comparison with work conducted by An et al. An's simulation modelled glass beads vibrated by a plate in three dimensions with periodic boundary conditions in the x and y axis (Yu et al., 2006). The packing density of the bed was calculated between $1/4Z_{max}$ and $3/4Z_{max}$, where Z_{max} was the height of settled particles at the time of calculating the packing density (An et al., 2005). Only the middle slice of the bed was analysed to avoid the structure imparted by the base or heaping of particles in the upper layers of the bed yielding a packing density unrepresentative of the bed's continuous phase. Any influence of side walls on the packing density was omitted through the implementation of periodic boundary conditions in the horizontal directions (Yu et al., 2006). It is unclear how exactly the packing density was calculated within this region however, this paper assumes that the number of sphere centres that lie between the plates were counted, and the volume of these spheres divided by the volume of the region between $1/4Z_{max}$ and $3/4Z_{max}$ yielded the packing density. The model parameters are in line with the default values shown in Table 1 of the work by An et al. (2008) with the exception that a typical coefficient of restitution of 0.922 ± 0.021 for glass beads was used instead of An's proposed damping coefficient of $2 \times 10^{-5}s$ (Lorenz et al., 1997). Preliminary simulations across a range of particle-particle coefficients of restitution showed no significant effect. The parameters used for the model's validation can be found in Table 1.

In accordance with the work conducted by An et al. (2008) and Yu et al. (2006), four methods of differing fill and vibration operation were investigated. The simulation parameters outlined in Table 1 were consistent throughout all experiments unless explicitly stated otherwise. Method 1: 3000 particles were dumped into

Table 1
Simulation parameters (An et al., 2008).

Simulation parameter	Value	Unit
Time step	7.9×10^{-6}	s
Number of particles	3000	-
Vibration amplitude	0.1d	m
Particle diameter (d)	0.01	m
Angular velocity (ω)	200	rad/s
Vibration frequency (f)	31.83	Hz
Particle density	2500	kg/m^3
Young's modulus	1×10^7	N/m^2
Poisson ratio	0.29	–
Particle-particle coefficient of sliding friction	0.3	–
Particle-wall coefficient of sliding friction	0.3	–
Particle-particle coefficient of rolling friction	0.002	–
Particle-wall coefficient of rolling friction	0.002	–
Particle-particle coefficient of restitution	0.922	–
Particle-wall coefficient of restitution	0.922	–
Particle-particle cohesion	0	–
Particle-wall cohesion	0	–
Particle drop height	0.3	m
Periodic boundary cuboid width	12d	m
Fixed boundary cylinder diameter	12d	m

the container within the first 2 s of simulation allowing more than enough time for all particles to enter the column, the particles were then vibrated for 12.5 s, vibration was then switched off and the particles left to settle for 1 s after which the final packing density was calculated. Method 2: 3000 particles were dumped into the container within the first 2 s of simulation allowing more than enough time for all particles to enter the column, the particles were then vibrated and relaxed in 0.5 s intervals over the course of 12.5 s, vibration was then switched off and the particles left to settle for 1 s after which the final packing density was calculated. Method 3: a batch of 98 particles was dropped every second onto an intermittently vibrating bed, vibrating for 1 s, still for 1 s, until 3000 particles were added; the bed ran under these vibration conditions for 58 s followed by 2 s of settling. Method 4: 3000 particles were dropped at a continuous rate of 98 particles/second onto an intermittently vibrating bed, vibrating for 1 s, still for 1 s; the bed ran under these vibration conditions for 58 s followed by 2 s of settling.

3. Results and analysis

3.1. Simulation/model validation

Methods 1 to 4 were performed with the simulation parameters outlined in Table 1. The data were then analysed via two procedures. Procedure 1 is the presumed packing density calculation in the work of An et al. (2008) and Yu et al. (2006). Packing density via procedure 1 was determined by simply counting the number of sphere centres between heights of $1/4Z_{max}$ and $3/4Z_{max}$ (An et al., 2005).

Procedure 2 for calculating the packing density involved voxelising the region between $1/4Z_{max}$ and $3/4Z_{max}$ and analysing the solid fraction within each voxel using KonigCell (Nicusan and Windows-Yule) (Powell & Abel, 2015). KonigCell is a high-performance library for rasterising particle locations onto a 2D or 3D Cartesian grid with arbitrarily high resolution. In 3D, as done in the present text, this is achieved by closely approximating a spherical particle as a polyhedron (the resolution of which can be increased based on the precision required) which is then recursively split across the Cartesian grid voxels - which are effectively boxes - that are intersected by the particle polyhedron, computing each particle-voxel intersection volume, even when the particle only partially covers the voxel. This intersection volume is then stored in each voxel of the Cartesian grid, such that after rasterising all particle locations we end up with an accurate solid fraction field irrespective of the grid resolution - in other words, the voxels can be made arbitrarily fine with the solid fraction becoming more accurate still. Importantly, KonigCell can work with spheres that lie partly within the domain. A more detailed description of KonigCell can be found within the documentation (Nicusan, 2021). The solid fraction in each cell/voxel of this grid is then analysed. The mean of the voxel solid fractions resulted in procedure 2's calculated packing density. Procedure 2 provides a more accurate representation of the true packing density of particles within the geometry as it removes the error present in procedure 1 imparted by being unable to distinguish, at the domains z axis boundary, the fraction of the particle that is within the domain. This results in procedure 1 overestimating the packing density. Due to procedure 2's more true-to-life representation of the packing density, procedure 2 will be used to calculate packing density for the remainder of the paper unless procedure 1 is explicitly referenced. Procedure 1 graphs can however be found in the appendix to allow a more direct comparison of this paper packing density results with those found in literature. The evolution in packing density, determined via procedure 2, vibrated in accordance with methods 1 and 2 can be seen in Figs. 1 and 2 respectively.

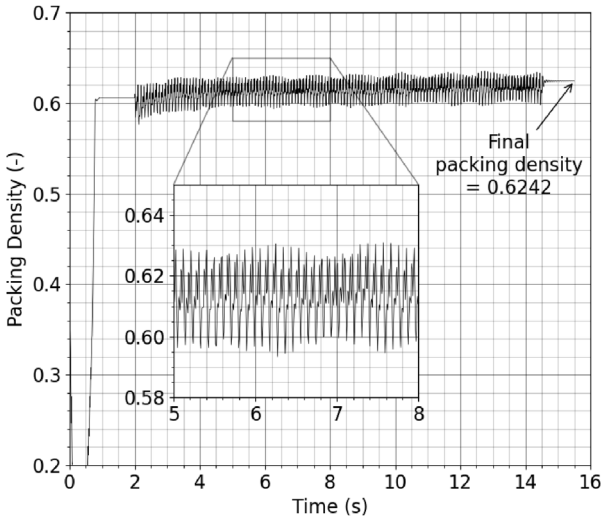

Fig. 1. Evolution of procedure 2 particle packing density with time under continuous vibration operation outlined in method 1.

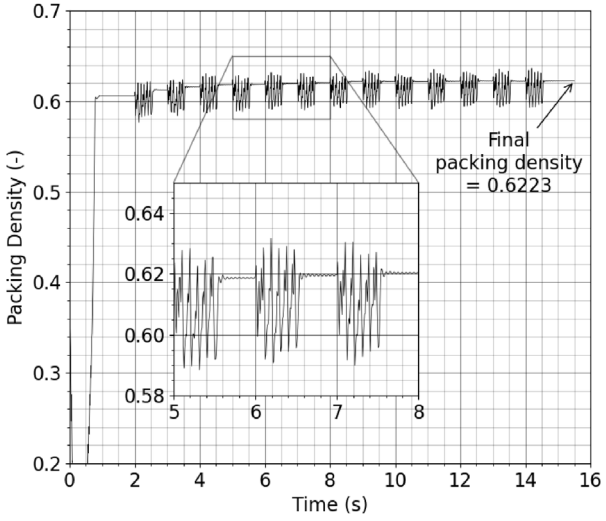

Fig. 2. Evolution of procedure 2 particle packing density with time under periodic vibration operation outlined in method 2.

To assess the validity of the DEM model, the final packing density values from the work of An et al. for packing methods 1 (An et al., 2008) and 2 (An et al., 2008) were plotted alongside this study's results, Fig. 3. To provide a more rigorous model validation, the final packing density values from the work of Yu et al. were plotted alongside this study's results for packing methods 3 (Yu et al., 2006) and 4 (Yu et al., 2006), Fig. 4. The spread of this study's results can be seen in the boxplots in Figs. 3 and 4, with each boxplot formed from 20 simulation repeats. The repeats only differed by the seed number dictating the arrangement of the particles prior to being dropped onto the plate. Procedure 2 packing density can also be seen in Figs. 3 and 4, providing useful proof of the overestimate in procedure 1. Procedure 2 also provides useful validation that the true packing density is not violating the maximal achievable packing density of 0.74048 outlined by the Kepler conjecture (Hales, 2005). Procedure 2's packing density shows a truer representation of the spread of data as is not prone to the uncertainty at z boundaries outlined above. The relative precision of procedure 2 and procedure 1 can be seen in Figs. 3 and 4. Figs. 3 and 4 show that the results from literature align with the

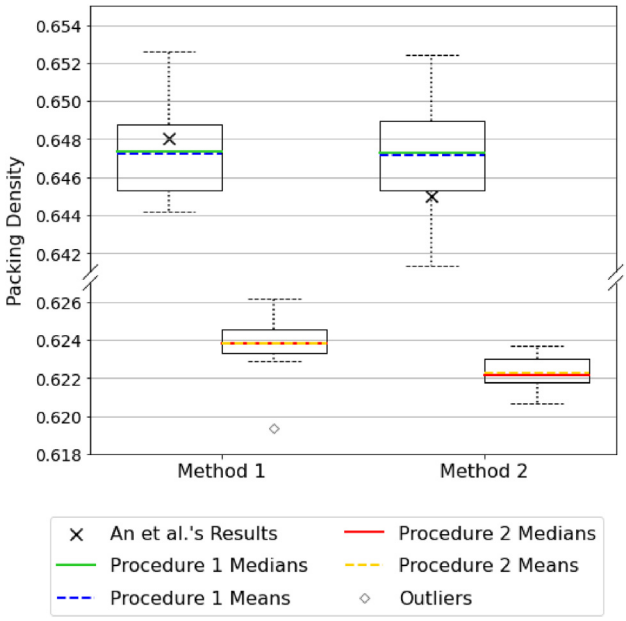

Fig. 3. Boxplot for packing methods 1 and 2, with each boxplot generated from 20 simulation repeats. The boxplot whiskers spread to the final point that lies within 1.5 interquartile ranges of the quartiles, The outliers are the points outside this range. The simulation results were compared against the work of An et al. (2008) (Dichter, 2020).

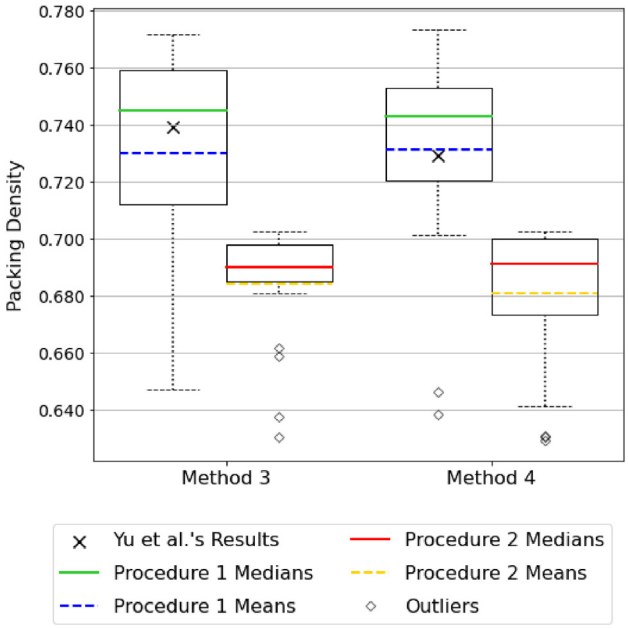

Fig. 4. Boxplot for packing methods 3 and 4, with each boxplot generated from 20 simulation repeats. The boxplot whiskers spread to the final point that lies within 1.5 interquartile ranges of the quartiles, The outliers are the points outside this range. The simulation results were compared against the work of Yu et al. (2006).

model packing density calculated via procedure 1, hence validating the packing model. Calculating the packing density between $1/4Z_{max}$ and $3/4Z_{max}$ was found to accurately capture a region of constant packing density within the bed, avoiding heaping and structuring of the base for all the repeats in Figs. 3 and 4, as shown in Fig. 5. Methods 3 and 4 can be seen to generate a more densely packed system. While this could be in small part attributed to the longer vibration time of the particles, this is decidedly not the sole cause of the differences between the methods. Running method 1

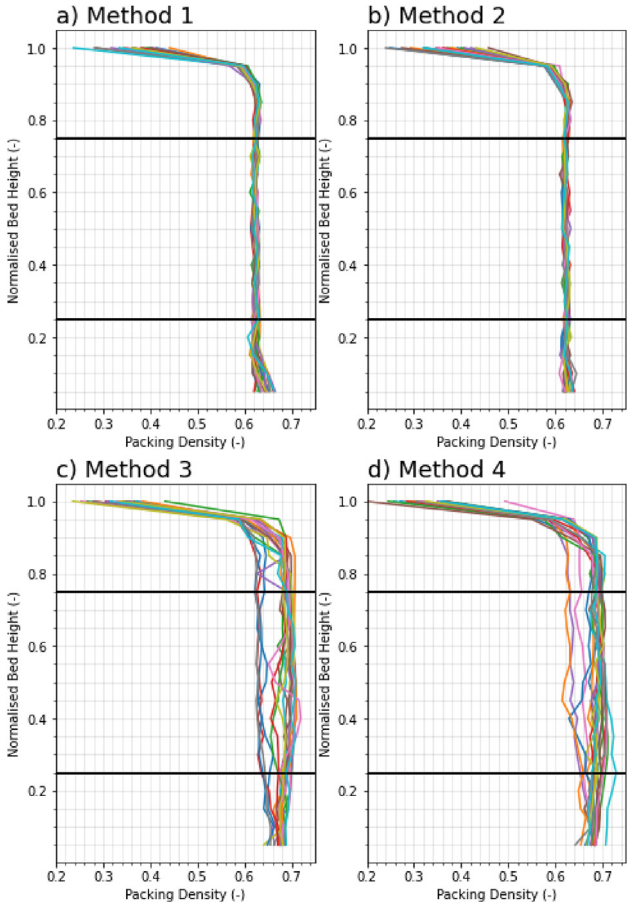

Fig. 5. Packing fraction up the bed calculated via procedure 2 for the data displayed in Figs. 3 and 4.

for 60 s as opposed to the 12.5 s of vibration displayed in Fig. 3 yields an average packing density of 0.6288 when calculated via procedure 2. This packing density is marginally higher than the average of 0.6238 when vibration only lasts for 12.5 s, though still markedly lower than the procedure 2 packing densities of 0.6839 and 0.6809 achieved by methods 3 and 4 respectively. The most noticeable difference of running procedure 1 for 60 s is that the spread of packing density repeats increases. As method 1 will not be compared to methods 3 and 4 within this paper but rather only the influence of particle-wall friction parameters analysed, and the difference in packing density due to increased vibration time is small compared to the difference between different methods, the differing vibration times do not have any meaningful impact on the results presented.

3.2. *Influence of wall properties*

To investigate the influence of the wall properties on the final packing density a cylindrical geometry with a diameter of 12d as outlined in Table 1 was chosen for the system in order to align with the work of An et al. (2008). The cylinder walls displayed fixed boundary conditions as opposed to the periodic boundary conditions applied during the model validation. The particle-wall coefficient of restitution, the particle-wall coefficient of rolling friction and the particle-wall coefficient of sliding friction were varied over the ranges displayed in Fig. 6, Figs. 7 and 8 with all other parameters the same as those outlined in Table 1. The cylinder walls were vibrated in accordance with the vibration method outlined in

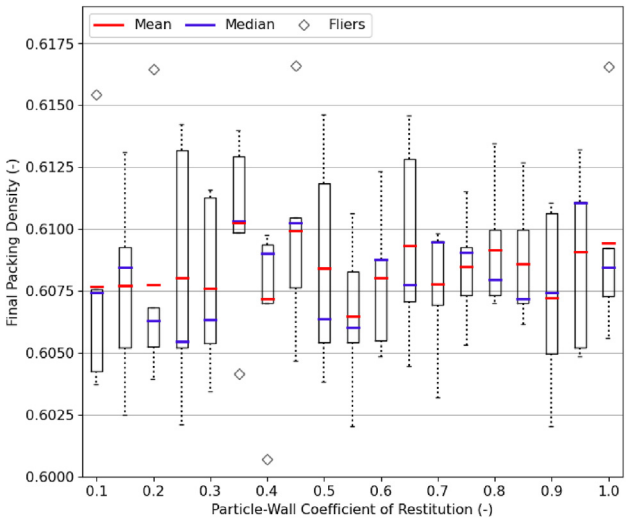

Fig. 6. Final packing density of glass beads in a cylinder of varying particle-wall coefficient of restitution. Each boxplot is generated from 5 repeats. Parameters of the particles and wall can be found in Table 1.

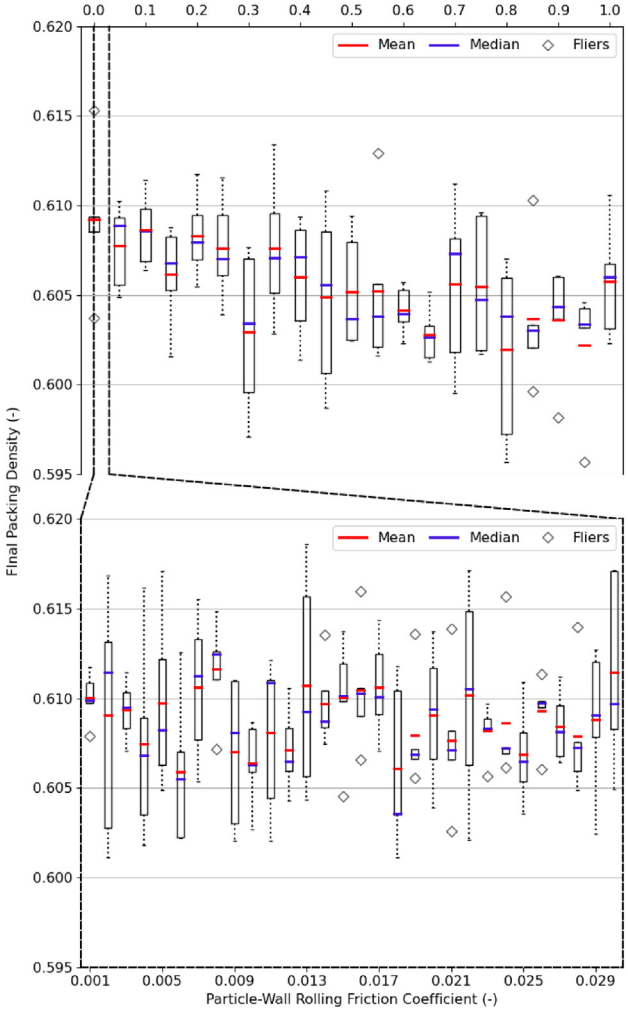

Fig. 7. Final packing density of glass beads in a cylinder of varying particle-wall coefficient of rolling friction. Each boxplot is generated from 5 repeats. Parameters of the particles and wall can be found in Table 1.

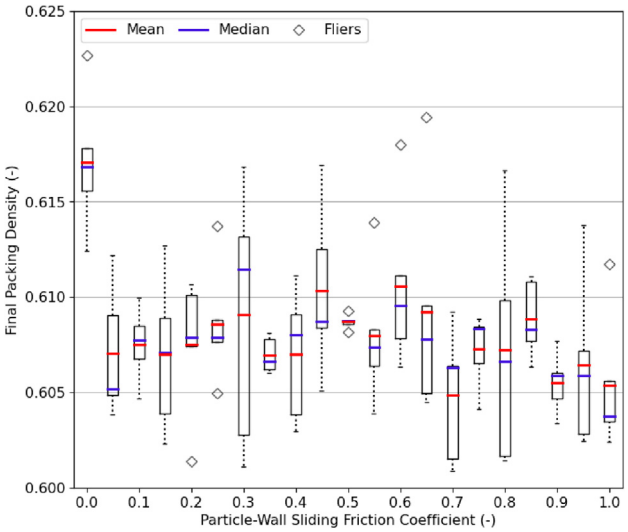

Fig. 8. Final packing density of glass beads in a cylinder of varying particle-wall coefficient of sliding friction. Each boxplot is generated from 5 repeats. Parameters of the particles and wall can be found in Table 1.

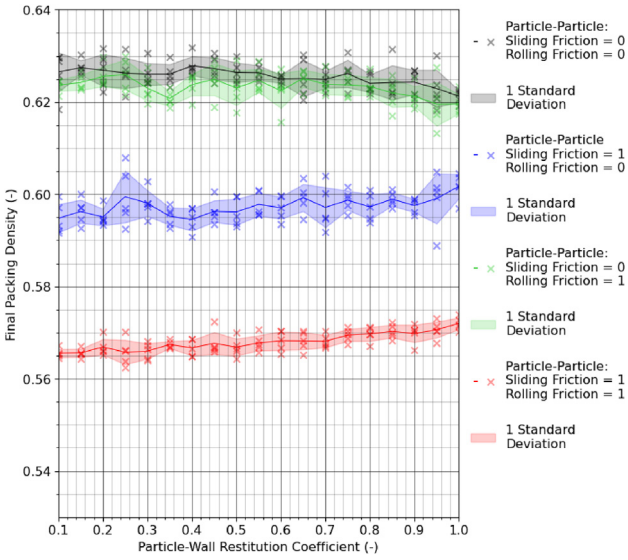

Fig. 9. Change in the final packing density of particles vibrated in accordance with method 1 for differing particle-wall coefficient of restitution. Each particle-wall coefficient of restitution has been investigated five times with differing random particle arrangements prior to dumping into the cylinder.

method 1 and the packing density calculated via procedure 2. Five repeats were performed for each set of simulation parameters, with the repeated simulations differing only in the seed number that dictated the arrangement of the particles prior to being dropped into the cylinder. Figs. 6, Figs. 7 and 8 show the wall properties to have negligible influence on the final packing density of glass beads vibrated in accordance with method 1. In many ways, this result is positive as it suggests that when dealing with reasonably smooth particles changes in the container material will not affect the packing density of the particles. It is however important to test the generality of this observation beyond the specific set of parameters used for our model validation. To assess the generality of our findings the next step of the study was to investigate if the wall

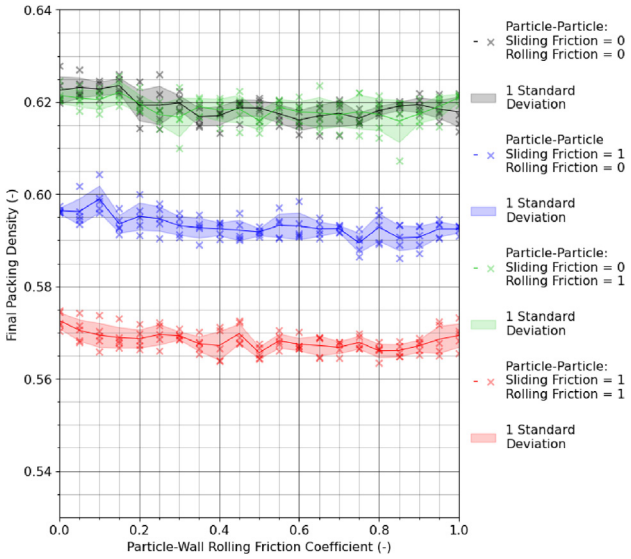

Fig. 10. Change in the final packing density of particles vibrated in accordance with method 1 for differing particle-wall coefficient of rolling friction. Each particle-wall coefficient of restitution has been investigated five times with differing random particle arrangements prior to dumping into the cylinder.

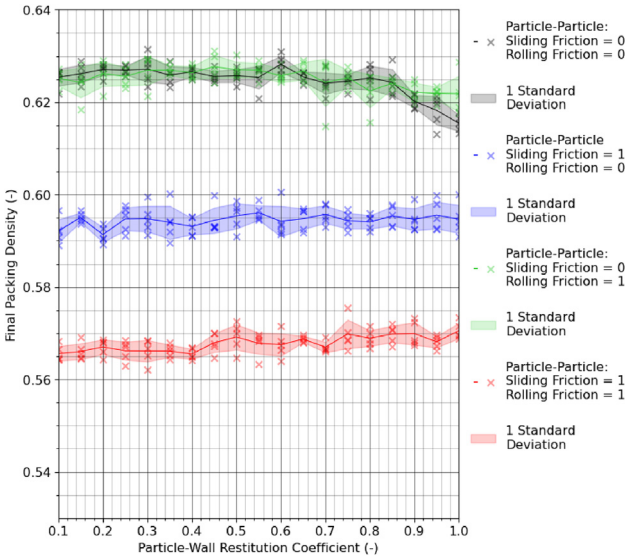

Fig. 12. Change in the final packing density of particles vibrated in accordance with method 2 for differing particle-wall coefficient of restitution. Each particle-wall coefficient of restitution has been investigated five times with differing random particle arrangements prior to dumping into the cylinder.

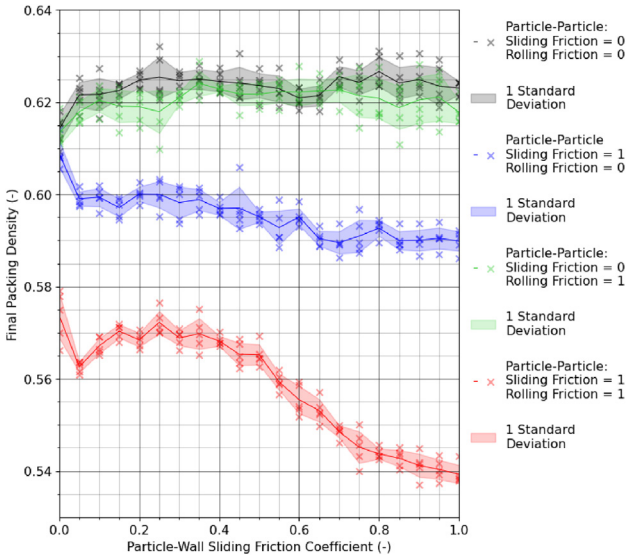

Fig. 11. Change in the final packing density of particles vibrated in accordance with method 1 for differing particle-wall coefficient of sliding friction. Each particle-wall coefficient of restitution has been investigated five times with differing random particle arrangements prior to dumping into the cylinder.

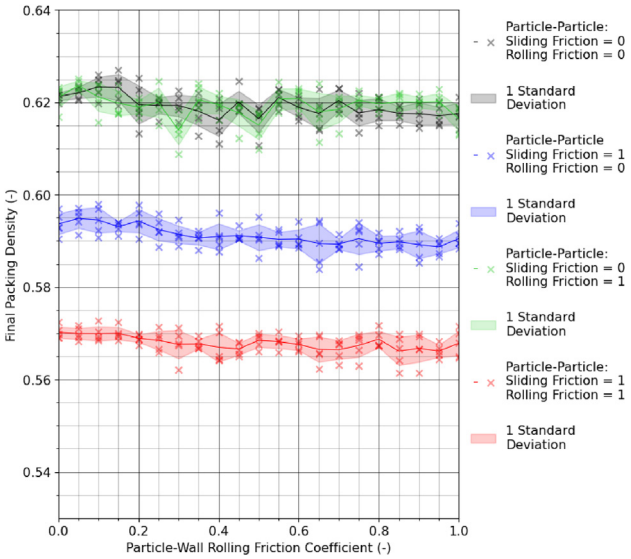

Fig. 13. Change in the final packing density of particles vibrated in accordance with method 2 for differing particle-wall coefficient of rolling friction. Each particle-wall coefficient of restitution has been investigated five times with differing random particle arrangements prior to dumping into the cylinder.

properties still had negligible impact when the particle-particle friction properties were changed.

Figs. 9, 10 and 11 show the response of final packing density to a change in particle-wall coefficient of restitution, coefficient of rolling friction and coefficient of sliding friction respectively for particles vibrated in accordance with method 1. Fig. 9 shows a minor increase in the final packing density with particle-wall coefficient of restitution when the particle-particle coefficient of sliding friction = 1. A possible reasoning for this could be that a higher particle-wall coefficient of restitution results in less velocity lost from a particle on collision with the container walls and hence more kinetic energy remains in the system to promote particle rearrangement. The positive gradient in Fig. 9 is however small compared to the uncertainty gained from the repeats at different particle arrangements prior to dropping and hence no statistically significant conclusions can be drawn other than that the particle-wall coefficient of restitution has negligible effect on the final packing density of particles. Fig. 10 shows an increase in particle-wall coefficient of rolling friction to minorly decrease the final packing density of particles over the range of particle-particle friction parameters though again not to a statistically significant degree. Finally, Fig. 11 shows the particle-wall coefficient of sliding friction to have no effect on the final packing density of the particles when the particle-particle coefficient of sliding friction = 0. However, when the particle-particle coefficient of sliding friction = 1 and the particle-particle coefficient of rolling friction = 0 there is a

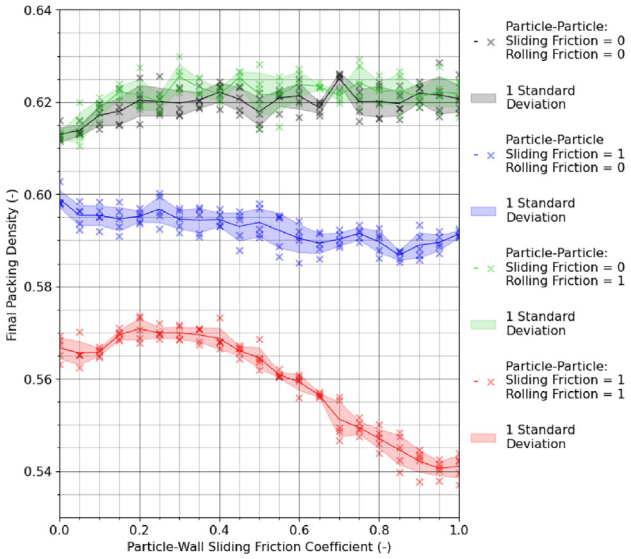

Fig. 14. Change in the final packing density of particles vibrated in accordance with method 2 for differing particle-wall coefficient of sliding friction. Each particle-wall coefficient of restitution has been investigated five times with differing random particle arrangements prior to dumping into the cylinder.

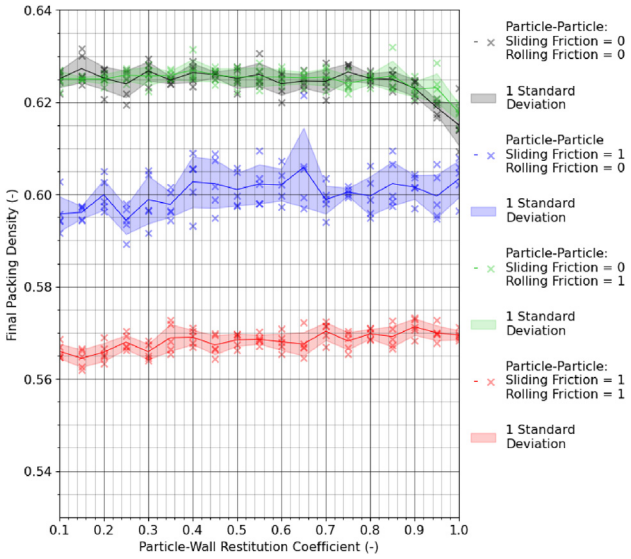

Fig. 15. Change in the final packing density of particles vibrated in accordance with method 3 for differing particle-wall coefficient of restitution. Each particle-wall coefficient of restitution has been investigated five times with differing random particle arrangements prior to dumping into the cylinder.

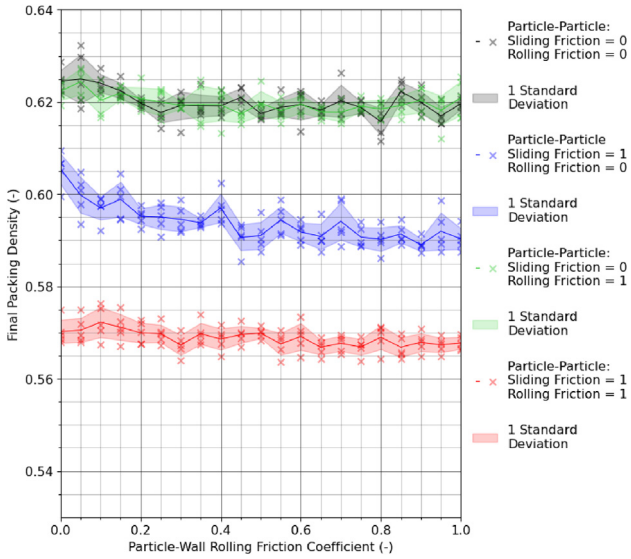

Fig. 16. Change in the final packing density of particles vibrated in accordance with method 3 for differing particle-wall coefficient of rolling friction. Each particle-wall coefficient of restitution has been investigated five times with differing random particle arrangements prior to dumping into the cylinder.

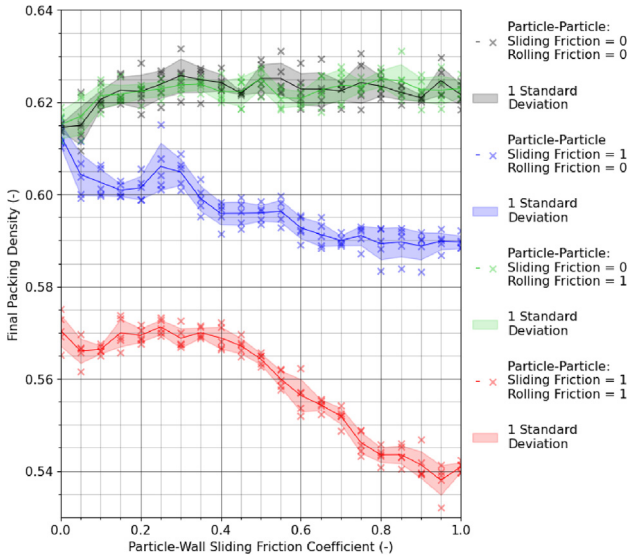

Fig. 17. Change in the final packing density of particles vibrated in accordance with method 3 for differing particle-wall coefficient of sliding friction. Each particle-wall coefficient of restitution has been investigated five times with differing random particle arrangements prior to dumping into the cylinder.

noticeable decrease in final packing density with an increase in the particle-wall coefficient of sliding friction. The greatest effect in Fig. 11 can be seen when the particle-particle coefficient of sliding friction = 1 and the particle-particle coefficient of rolling friction = 1, for this case there is a significant decrease in the final packing density of particles with increasing particle-wall coefficient of sliding friction. The system behaviour shown in Fig. 11 can be attributed to the propagation of force chains throughout the cylinder as the particle-particle friction increases. These frictional force chains result in particle jamming that limits the effectiveness of the vibration rearranging the particles into a denser arrangement and results in a lower packing density. A study into the packing of jammed particles can be found in the work of Torquato and Stillinger (2010). The next step of the study was to investigate if the behaviour exhibited by the particles in Figs. 9, 10 and 11 differed when the particles were added to the cylinder in accordance with methods 2, 3 and 4.

The first thing to note with Fig. 12–20 is that the packing densities are remarkably similar to those of Fig. 9, Figs. 10 and 11 where the particles were vibrated in accordance with method 1. This may initially seem unexpected with the model validation determining the packing densities of methods 3 and 4 to be significantly higher than those of method 1 however, this behaviour is in agreement with the literature. Experiments conducted by Yu et al. (2006) found the batch packing method to be much more sensitive to a decrease in the ratio of the diameter of the particles to the diameter

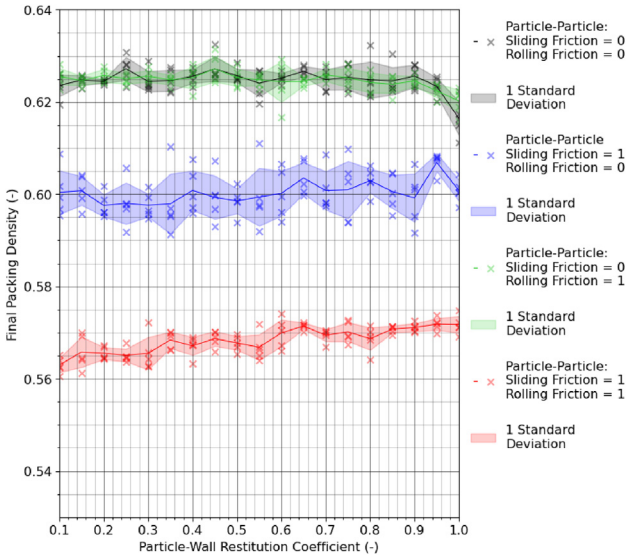

Fig. 18. Change in the final packing density of particles vibrated in accordance with method 4 for differing particle-wall coefficient of restitution. Each particle-wall coefficient of restitution has been investigated five times with differing random particle arrangements prior to dumping into the cylinder.

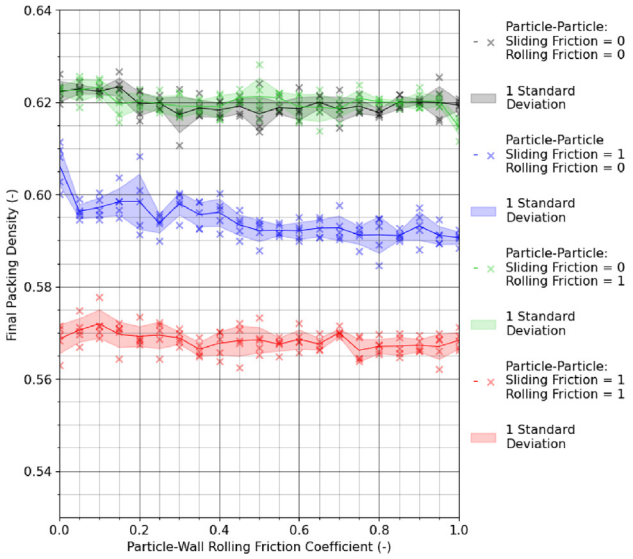

Fig. 19. Change in the final packing density of particles vibrated in accordance with method 4 for differing particle-wall coefficient of rolling friction. Each particle-wall coefficient of restitution has been investigated five times with differing random particle arrangements prior to dumping into the cylinder.

of the cylinder (d/D ratio). Extrapolating Yu and An et al.'s lines to this study d/D ratio of 1/12 the final packing densities for methods 1 and 2 and methods 3 and 4 are very similar, hence explaining the similarity in final packing density witnessed in Fig. 9–20

In alignment with the results for vibration in accordance with method 1 seen in Fig. 9 an increase in particle-wall coefficient of restitution, shown in Fig. 12, Figs. 15 and 18 for methods 2, 3 and 4 respectively, yields minor increases in final packing density when the particle-particle coefficient of sliding friction = 1. The increases, however, as with the increase for method 1 shown in Fig. 9, are not to a statistically significant degree. The effect of particle-wall coefficient of rolling friction for methods 2, 3 and 4, shown in Fig. 13, Figs. 16 and 19 respectively shows a minor decrease in final packing

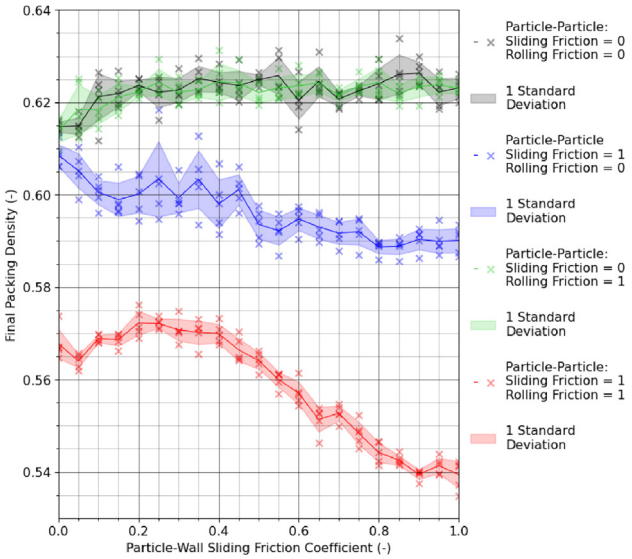

Fig. 20. Change in the final packing density of particles vibrated in accordance with method 4 for differing particle-wall coefficient of sliding friction. Each particle-wall coefficient of restitution has been investigated five times with differing random particle arrangements prior to dumping into the cylinder.

density with the increase in particle-wall coefficient of rolling friction when the particle-particle coefficient of sliding friction = 1. The magnitude of drop in final packing density for vibration in accordance with methods 2, 3 and 4 is similar to the magnitude of drop in final packing density for vibration in accordance with method 1. The decreases, however, as with the decrease for method 1 shown in Fig. 10, are not to a statistically significant degree. Finally, the coefficient of sliding friction can be seen in Fig. 14, 17 and 20 to cause a significant decrease in the final packing density of particles when the coefficient of sliding friction = 1. The magnitude of the decreases in packing density is comparable to the decrease for method 1 vibration shown in Fig. 11. These decreases as mentioned above can be put down to the propagation of force chains throughout the packing limiting the effectiveness of rearrangement via vibration.

4. Conclusions

In this paper, we have used DEM to explore the influence of material wall properties on the behaviours of three-dimensionally vibrated granular packings of spherical particles. All the code files used within this paper can be found on Github: https://github.com/Jack-Grogan/DEM-Vibropacking-Wall-Effects. For particles possessing low to moderate interparticle friction coefficients, the material properties of the vessel were found to have little to no influence on the packing behaviour of said particles. For high values of interparticle friction, however, the influence of the wall properties became more pronounced. Increases in particle-wall coefficient of restitution were seen to result in a minor increase in packing density when the particle-particle coefficient of sliding friction = 1 for all methods 1, 2, 3 and 4, Fig. 9, Fig. 12, Figs. 15 and 18 respectively. This increase, however, was not to a statistically significant degree. Increases in the particle-wall coefficient of rolling friction were seen to minorly decrease the final packing density of particles with a particle-particle coefficient of sliding friction = 1 for all methods 1, 2, 3 and 4. This decrease as with the effect of particle-wall coefficient of restitution was to too little a degree to be distinguishable from the random error in the repeats. Finally, the study found that the particle-wall coefficient of sliding friction

caused a significant decrease in packing density for all methods 1, 2, 3 and 4 when the particle-particle coefficient of sliding friction = 1. This decrease was attributed to force chains propagating through the spheres limiting the rearrangement of particles with vibration. For particle packing of high sliding friction particles, the friction properties of the wall, especially the particle-wall coefficient of sliding friction, plays a major role in the final packing density of mono-disperse spheres. The paper's findings stress the need to choose an appropriate vessel material to optimise packing of particles with a high particle-particle coefficient sliding friction. However, if particles have low to moderate values of interparticle friction coefficients, packing behaviour is largely agnostic to wall properties. This result is good news for the industry, as it removes constraints on the allowable container materials to achieve a desirable packing density.

Declaration of interest

The authors declare that they have no known competing financial interests or personal relationships that could have appeared to influence the work reported in this paper.

Acknowledgements

This work could not have been completed without the support of Dominik Werner, Aaron Wiggin, Daniel Rhymer and William Peace. The computation work described in this paper was performed using the University of Birmingham's high-performance computer: BlueBEAR. BlueBEAR provides a high-performance computing service to the University of Birmingham's research community. More information regarding BlueBEAR can be found online (University of Birmingham, 2023).

Appendix

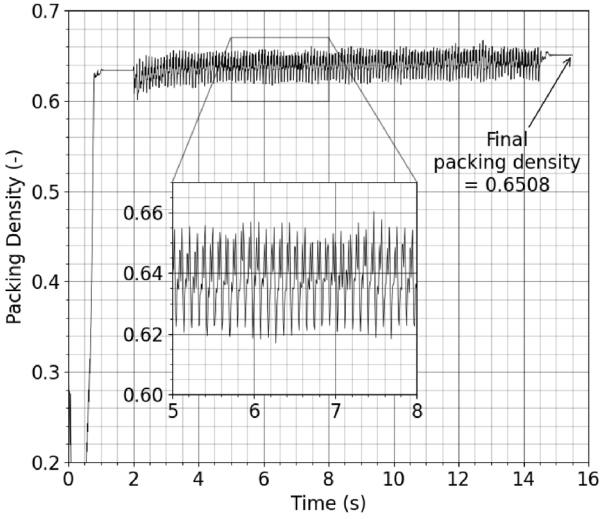

Fig. 21. Evolution of procedure 1 particle packing density with time under continuous vibration operation outlined in method 1.

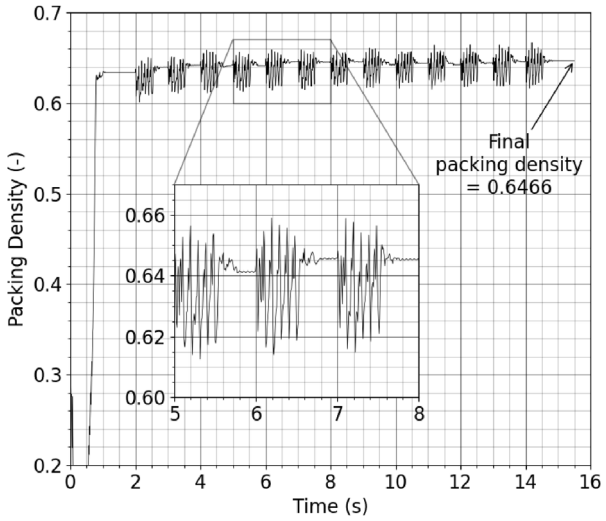

Fig. 22. Evolution of procedure 1 particle packing density with time under periodic vibration operation outlined in method 2.

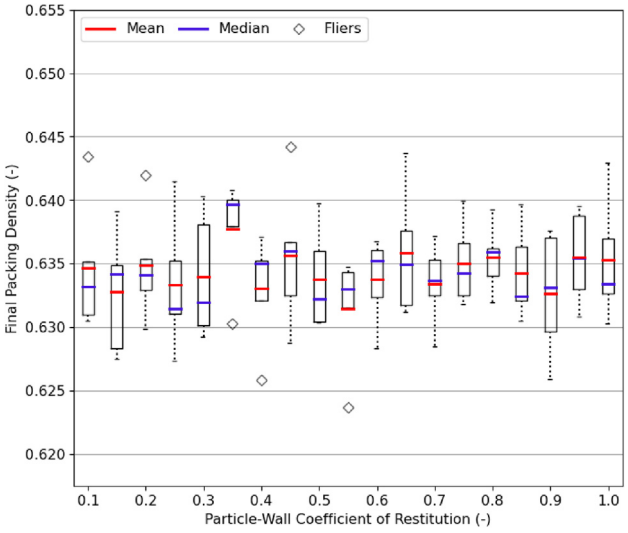

Fig. 23. Final packing density of glass beads in a cylinder of varying particle-wall coefficient of restitution. Each boxplot is generated from 5 repeats. Parameters of the particles and wall can be found in Table 1.

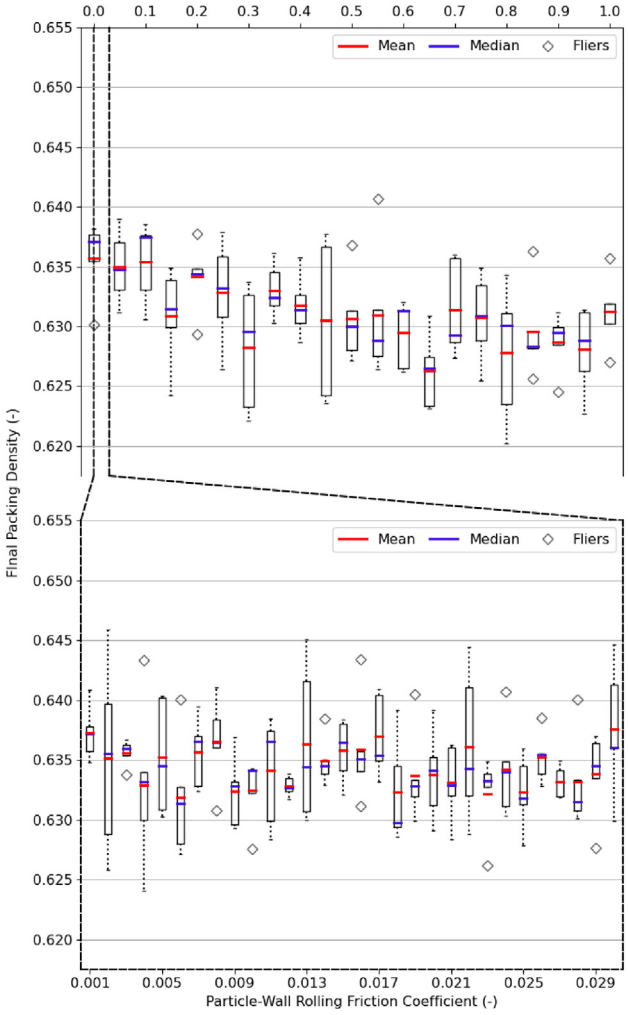

Fig. 24. Final packing density of glass beads in a cylinder of varying particle-wall coefficient of rolling friction. Each boxplot is generated from 5 repeats. Parameters of the particles and wall can be found in Table 1.

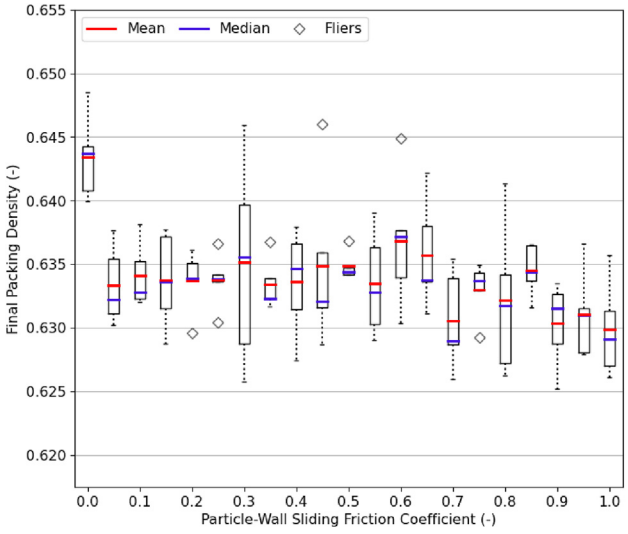

Fig. 25. Final packing density of glass beads in a cylinder of varying particle-wall coefficient of sliding friction. Each boxplot is generated from 5 repeats. Parameters of the particles and wall can be found in Table 1.

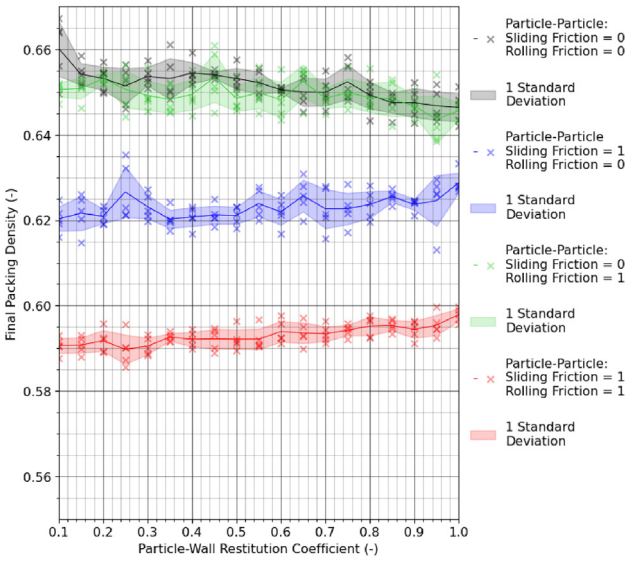

Fig. 26. Change in the final packing density of particles vibrated in accordance with method 1 for differing particle-wall coefficient of restitution. Each particle-wall coefficient of restitution has been investigated five times with differing random particle arrangements prior to dumping into the cylinder.

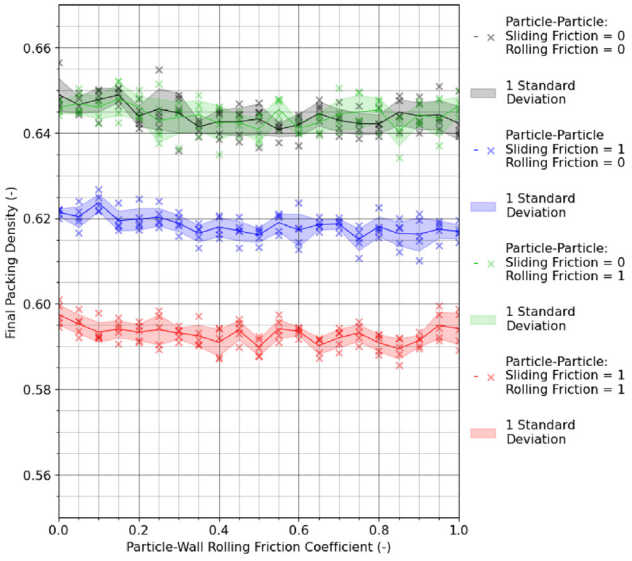

Fig. 27. Change in the final packing density of particles vibrated in accordance with method 1 for differing particle-wall coefficient of rolling friction. Each particle-wall coefficient of restitution has been investigated five times with differing random particle arrangements prior to dumping into the cylinder.

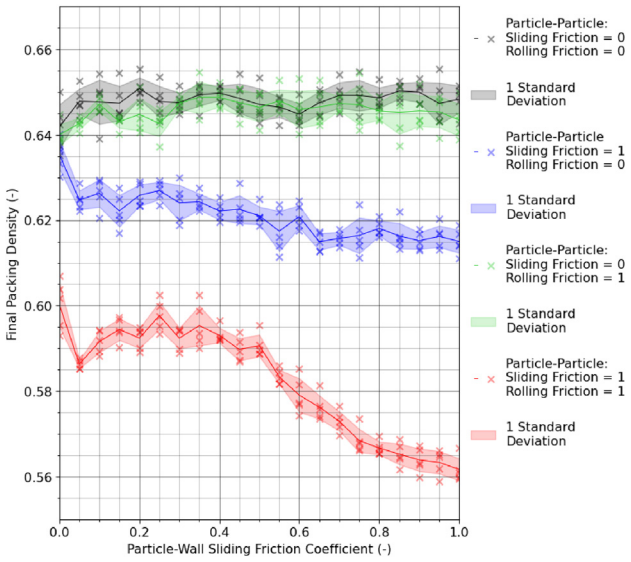

Fig. 28. Change in the final packing density of particles vibrated in accordance with method 1 for differing particle-wall coefficient of sliding friction. Each particle-wall coefficient of restitution has been investigated five times with differing random particle arrangements prior to dumping into the cylinder.

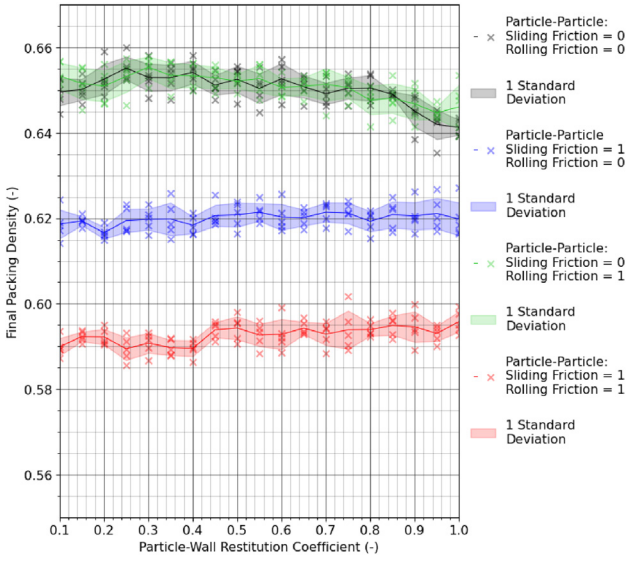

Fig. 29. Change in the final packing density of particles vibrated in accordance with method 2 for differing particle-wall coefficient of restitution. Each particle-wall coefficient of restitution has been investigated five times with differing random particle arrangements prior to dumping into the cylinder.

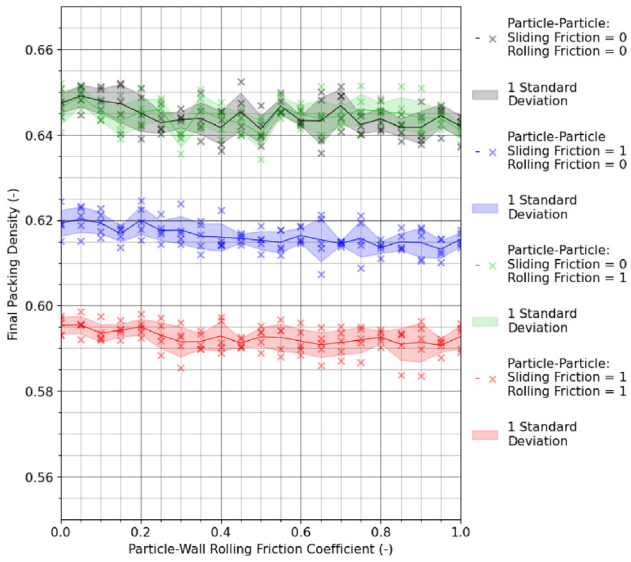

Fig. 30. Change in the final packing density of particles vibrated in accordance with method 2 for differing particle-wall coefficient of rolling friction. Each particle-wall coefficient of restitution has been investigated five times with differing random particle arrangements prior to dumping into the cylinder.

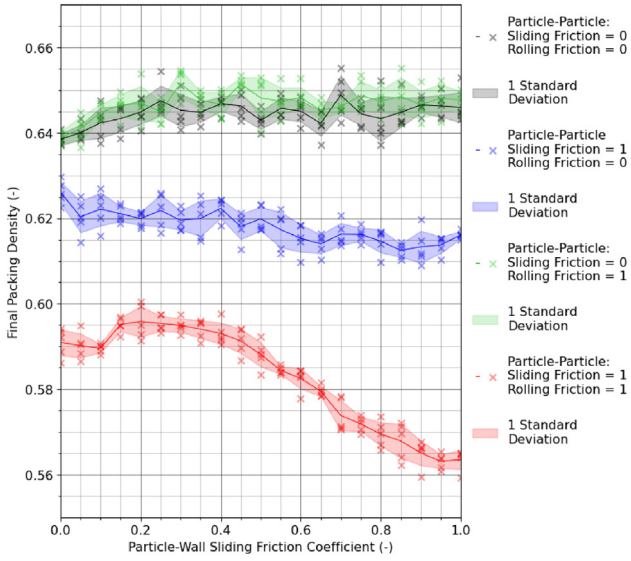

Fig. 31. Change in the final packing density of particles vibrated in accordance with method 2 for differing particle-wall coefficient of sliding friction. Each particle-wall coefficient of restitution has been investigated five times with differing random particle arrangements prior to dumping into the cylinder.

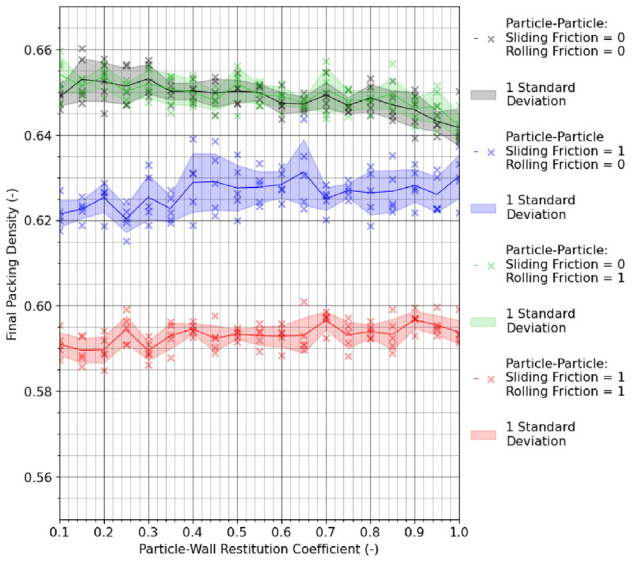

Fig. 32. Change in the final packing density of particles vibrated in accordance with method 3 for differing particle-wall coefficient of restitution. Each particle-wall coefficient of restitution has been investigated five times with differing random particle arrangements prior to dumping into the cylinder.

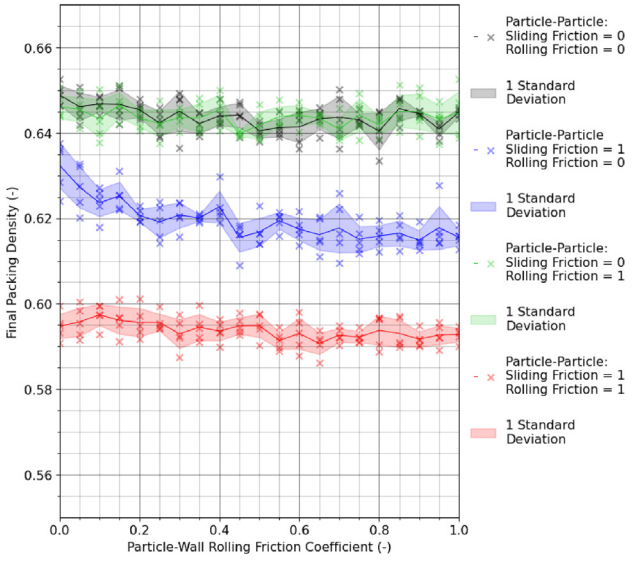

Fig. 33. Change in the final packing density of particles vibrated in accordance with method 3 for differing particle-wall coefficient of rolling friction. Each particle-wall coefficient of restitution has been investigated five times with differing random particle arrangements prior to dumping into the cylinder.

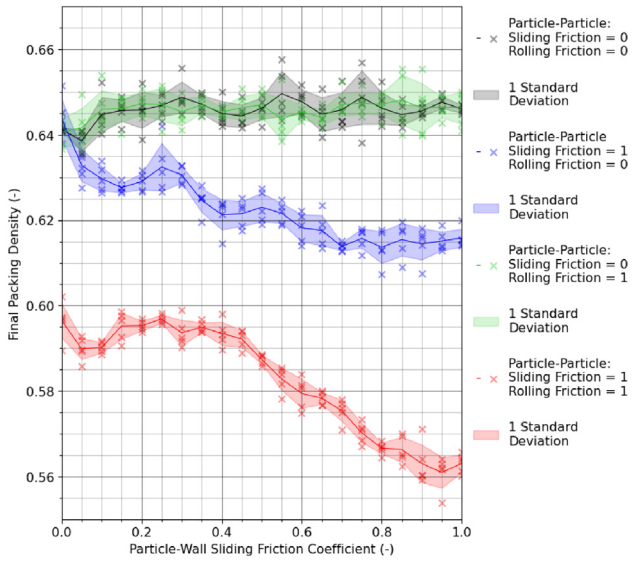

Fig. 34. Change in the final packing density of particles vibrated in accordance with method 3 for differing particle-wall coefficient of sliding friction. Each particle-wall coefficient of restitution has been investigated five times with differing random particle arrangements prior to dumping into the cylinder.

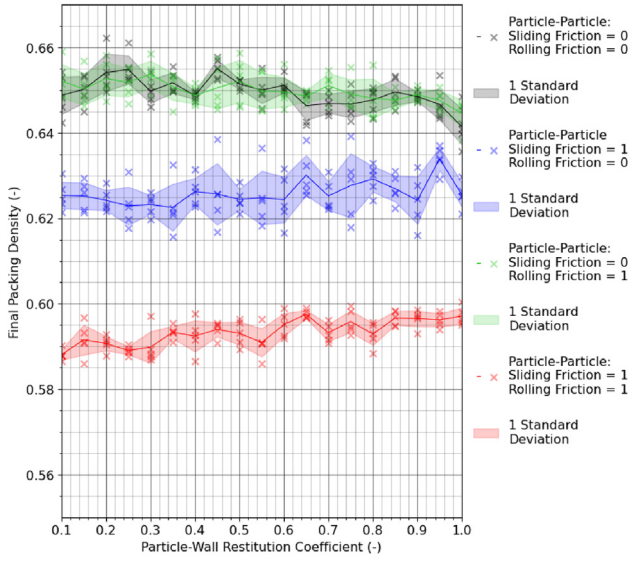

Fig. 35. Change in the final packing density of particles vibrated in accordance with method 4 for differing particle-wall coefficient of restitution. Each particle-wall coefficient of restitution has been investigated five times with differing random particle arrangements prior to dumping into the cylinder.

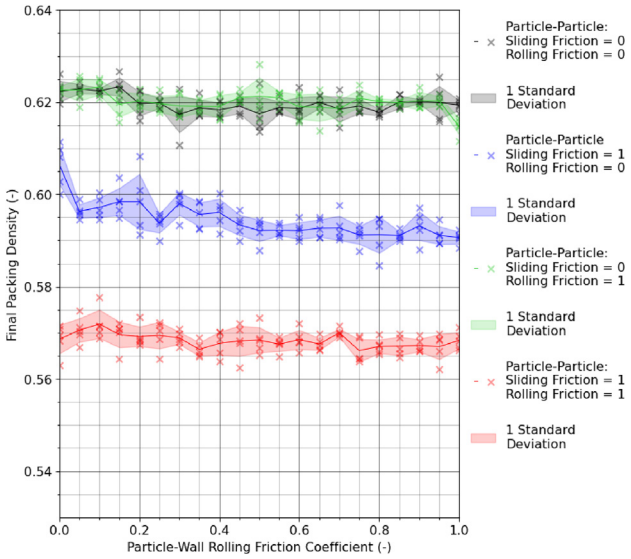

Fig. 36. Change in the final packing density of particles vibrated in accordance with method 4 for differing particle-wall coefficient of rolling friction. Each particle-wall coefficient of restitution has been investigated five times with differing random particle arrangements prior to dumping into the cylinder.

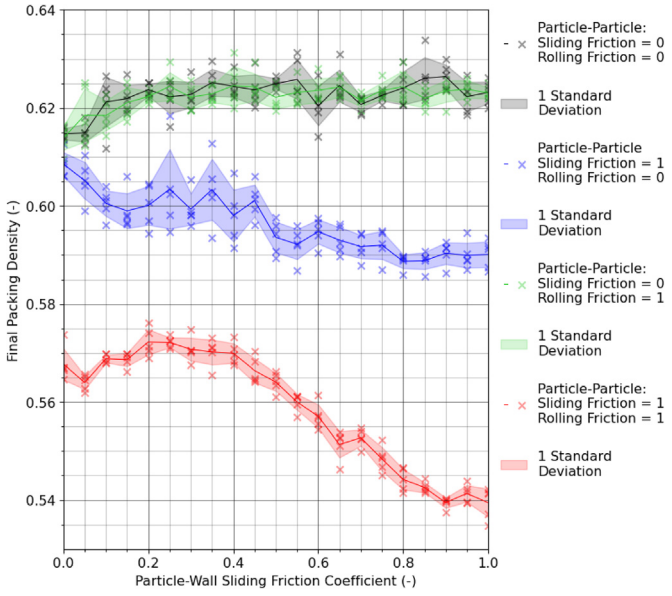

Fig. 37. Change in the final packing density of particles vibrated in accordance with method 4 for differing particle-wall coefficient of sliding friction. Each particle-wall coefficient of restitution has been investigated five times with differing random particle arrangements prior to dumping into the cylinder.

References

An, X., & Chai, H. (2016). Packing densification of binary cylindrical particle mixtures under 3d mechanical vibrations. *Advanced Powder Technology, 27*(6), 2489–2495. https://doi.org/10.1016/j.apt.2016.09.024. https://www.sciencedirect.com/science/article/pii/S0921883116302722

An, X., He, S., Feng, H., & Qian, Q. (2015). Packing densification of binary mixtures of spheres and cubes subjected to 3d mechanical vibrations. *Applied Physics A, 118*, 151–162.

An, X., & Li, C. (2013). Experiments on densifying packing of equal spheres by two-dimensional vibration. *Particuology, 11*(6), 689–694. https://doi.org/10.1016/j.partic.2012.06.019. https://www.sciencedirect.com/science/article/pii/S1674200113000746

An, X., Li, C., & Qian, Q. (2016). Experimental study on the 3d vibrated packing densification of binary sphere mixtures. *Particuology, 27*, 110–114. https://doi.org/10.1016/j.partic.2015.03.009. https://www.sciencedirect.com/science/article/pii/S1674200115001492

An, X., Li, C., Yang, R., Zou, R., & Yu, A. (2009). Experimental study of the packing of mono-sized spheres subjected to one-dimensional vibration. *Powder Technology, 196*(1), 50–55. https://doi.org/10.1016/j.powtec.2009.06.016. https://www.sciencedirect.com/science/article/pii/S0032591009004008. URL.

An, X. Z., Yang, R. Y., Dong, K. J., Zou, R. P., & Yu, A. B. (2005). Micromechanical simulation and analysis of one-dimensional vibratory sphere packing. *Physical Review Letters, 95*, Article 205502. https://doi.org/10.1103/PhysRevLett.95.205502. https://link.aps.org/doi/10.1103/PhysRevLett.95.205502

An, X., Yang, R., Zou, R., & Yu, A. (2008). Effect of vibration condition and inter-particle frictions on the packing of uniform spheres. *Powder Technology, 188*(2), 102–109. https://doi.org/10.1016/j.powtec.2008.04.001. https://www.sciencedirect.com/science/article/pii/S0032591008001757

Ayer, J. E., & Soppet, F. E. (1965). Vibratory compaction: I, compaction of spherical shapes. *Journal of the American Ceramic Society, 48*(4), 180–183. https://doi.org/10.1111/j.1151-2916.1965.tb14708.x. arXiv:https://ceramics.onlinelibrary.wiley.com/doi/pdf/10.1111/j.1151-2916.1965.tb14708.x https://ceramics.onlinelibrary.wiley.com/doi/abs/10.1111/j.1151-2916.1965.tb14708.x.

Dichter, B. (2020). *brokenaxis*. https://github.com/bendichter/brokenaxes/tree/master.

Hales, T. C. (2005). A proof of the kepler conjecture. *Annals of Mathematics, 162*(3), 1065–1185. http://www.jstor.org/stable/20159940.

Hettiarachchi, H., & Mampearachchi, W. (2018). Effect of vibration frequency, size ratio and large particle volume fraction on packing density of binary spherical mixtures. *Powder Technology, 336*, 150–160. https://doi.org/10.1016/j.powtec.2018.05.049

Li, J., An, X., Wang, J., Zhao, H., Zou, R., Dong, K., & Gou, D. (2020). Experimental study on 3d vibrated packing densification of mono-sized dodecahedral particles. *Powder Technology, 367*, 703–712. https://doi.org/10.1016/j.powtec.2020.04.020. https://www.sciencedirect.com/science/article/pii/S0032591020303065

Li, C., An, X., Yang, R., Zou, R., & Yu, A. (2011). Experimental study on the packing of uniform spheres under three-dimensional vibration. *Powder Technology, 208*(3), 617–622. https://doi.org/10.1016/j.powtec.2010.12.029. https://www.sciencedirect.com/science/article/pii/S0032591011000143

Li, C., Zou, R., Pinson, D., Yu, A., & Zhou, Z. (2020). An experimental study of packing of ellipsoids under vibrations. *Powder Technology, 361*, 45–51. https://doi.org/10.1016/j.powtec.2019.10.115. https://www.sciencedirect.com/science/article/pii/S0032591019309441

Lorenz, A., Tuozzolo, C., & Louge, M. (1997). Measurements of impact properties of small, nearly spherical particles. *Experimental Mechanics, 37*, 292–298.

McGeary, R. (1961). Mechanical packing of spherical particles. *Journal of the American Ceramic Society, 44*(10), 513–522.

Nicusan, A. L. (2021). *Konigcell documentation*. https://konigcell.readthedocs.io/en/latest/index.html.

Nicusan, A. L., & Windows-Yule, C.. Konigcell: Quantitative, fast grid-based fields calculations in 2d and 3d. https://github.com/anicusan/KonigCell,version=0.2.0 (2022-12-22).

Oman, A., & Watson, K. (1944). Pressure drops in granular beds. *National Petroleum News, 36*, R795–R802.

Powell, D., & Abel, T. (2015). An exact general remeshing scheme applied to physically conservative voxelization. *Journal of Computational Physics, 297*, 340–356. https://doi.org/10.1016/j.jcp.2015.05.022. https://www.sciencedirect.com/science/article/pii/S0021999115003563

Qian, Q., An, X., Wang, Y., Wu, Y., & Wang, L. (2016). Physical study on the vibrated packing densification of mono-sized cylindrical particles. *Particuology, 29*, 120–125. https://doi.org/10.1016/j.partic.2016.01.009. https://www.sciencedirect.com/science/article/pii/S1674200116300220

Qian, Q., Wang, L., An, X., Wu, Y., Wang, J., Zhao, H., & Yang, X. (2018). Dem simulation on the vibrated packing densification of mono-sized equilateral cylindrical particles. *Powder Technology, 325*, 151–160. https://doi.org/10.1016/j.powtec.2017.10.050. https://www.sciencedirect.com/science/article/pii/S0032591017308458

Reimann, J., Vicente, J., Brun, E., Ferrero, C., Gan, Y., & Rack, A. (2017). X-ray tomography investigations of mono-sized sphere packing structures in cylindrical containers. *Powder Technology, 318*, 471–483. https://doi.org/10.1016/j.powtec.2017.05.033. https://www.sciencedirect.com/science/article/pii/S0032591017304072

Rosato, A. D., & Windows-Yule, C. (2020). *Segregation in vibrated granular systems*. Academic Press.

Roskilly, S. J., Colbourn, E. A., Alli, O., Williams, D., Paul, K. A., Welfare, E. H., & Trusty, P. A. (2010). Investigating the effect of shape on particle segregation using a Monte Carlo simulation. *Powder Technology, 203*(2), 211–222.

Salamat, A., Golman, B., & Spitas, C. (2022). Effect of horizontal vibrations and particle size on the packing density of multi-sized sphere mixtures: Discrete element method simulation. *Journal of Manufacturing Science and Engineering, 144*(12), Article 121013.

Scott, G. D. (1960). Packing of spheres: Packing of equal spheres. *Nature, 188*(4754), 908–909.

Scott, G. D., & Kilgour, D. M. (1969). The density of random close packing of spheres. *Journal of Physics D: Applied Physics, 2*(6), 863. https://doi.org/10.1088/0022-3727/2/6/311

Torquato, S., & Stillinger, F. H. (2010). Jammed hard-particle packings: From kepler to bernal and beyond. *Reviews of Modern Physics, 82*, 2633–2672. https://

doi.org/10.1103/RevModPhys.82.2633. https://link.aps.org/doi/10.1103/RevModPhys.82.2633

University of Birmingham, Birmingham environment for academic research (bear).(2023). https://intranet.birmingham.ac.uk/it/teams/infrastructure/research/bear/index.aspx. (Accessed 23 September 2023).

Wang, L., An, X., Wu, Y., Qian, Q., Zou, R., & Dong, K. (2021). Dem simulation of vibrated packing densification of mono-sized regular octahedral particles. *Powder Technology, 384*, 29–35. https://doi.org/10.1016/j.powtec.2021.02.007. https://www.sciencedirect.com/science/article/pii/S0032591021001108

White, H. E., & Walton, S. F. (1937). Particle packing and particle shape. *Journal of the American Ceramic Society, 20*(1–12), 155–166. https://doi.org/10.1111/j.1151-2916.1937.tb19882.x. arXiv:https://ceramics.onlinelibrary.wiley.com/doi/pdf/10.1111/j.1151-2916.1937.tb19882.x https://ceramics.onlinelibrary.wiley.com/doi/abs/10.1111/j.1151-2916.1937.tb19882.x.

Windows-Yule, C., Lanchester, E., Madkins, D., & Parker, D. (2018). New insight into pseudo-thermal convection in vibrofluidised granular systems. *Scientific Reports, 8*(1), Article 12859.

Windows-Yule, C., & Neveu, A. (2022). Calibration of dem simulations for dynamic particulate systems. *Papers in Physics, 14*, 140010. –140010.

Windows-Yule, C., Rivas, N., & Parker, D. (2013). Thermal convection and temperature inhomogeneity in a vibrofluidized granular bed: The influence of sidewall dissipation. *Physical Review Letters, 111*(3), Article 038001.

Windows-Yule, C., Rosato, A., Rivas, N., & Parker, D. (2014). Influence of initial conditions on granular dynamics near the jamming transition. *New Journal of Physics, 16*(6), Article 063016.

Windows-Yule, C., Tunuguntla, D. R., & Parker, D. (2016). Numerical modelling of granular flows: A reality check. *Computational particle mechanics, 3*, 311–332.

Windows-Yule, C. R. K., Weinhart, T., Parker, D. J., & Thornton, A. R. (2014). Effects of packing density on the segregative behaviors of granular systems. *Physical Review Letters, 112*, Article 098001. https://doi.org/10.1103/PhysRevLett.112.098001. URL https://link.aps.org/doi/10.1103/PhysRevLett.112.098001.

Wu, Y., An, X., & Yu, A. (2017). Dem simulation of cubical particle packing under mechanical vibration. *Powder Technology, 314*, 89. https://doi.org/10.1016/j.powtec.2016.09.029. –101, special Issue on Simulation and Modelling of Particulate Systems https://www.sciencedirect.com/science/article/pii/S0032591016305988. URL.

Xie, Z., An, X., Wu, Y., Wang, L., Qian, Q., & Yang, X. (2017). Experimental study on the packing of cubic particles under three-dimensional vibration. *Powder Technology, 317*, 13–22. https://doi.org/10.1016/j.powtec.2017.04.037. https://www.sciencedirect.com/science/article/pii/S0032591017303352. URL.

Yang, H., Li, S., Li, Z., & Ji, F. (2020). Experimental and numerical study on the packing densification of metal powder with gaussian distribution. *Metals, 10*(11). https://doi.org/10.3390/met10111401. https://www.mdpi.com/2075-4701/10/11/1401

Yu, A. (2004). Discrete element method: An effective way for particle scale research of particulate matter. *Engineering Computations, 21*(2/3/4), 205–214.

Yu, A. B., An, X. Z., Zou, R. P., Yang, R. Y., & Kendall, K. (2006). Self-assembly of particles for densest packing by mechanical vibration. *Physical Review Letters, 97*, Article 265501. https://doi.org/10.1103/PhysRevLett.97.265501. https://link.aps.org/doi/10.1103/PhysRevLett.97.265501

Yu, A., & Standish, N. (1993). A study of the packing of particles with a mixture size distribution. *Powder Technology, 76*(2), 113–124. https://doi.org/10.1016/S0032-5910(05)80018-X. https://www.sciencedirect.com/science/article/pii/S003259100580018X

Zhang, N. (2004). *Vibration-induced densification of granular materials*. New Jersey Institute of Technology.

Zhang, Z., Liu, L., Yuan, Y., & Yu, A. (2001). A simulation study of the effects of dynamic variables on the packing of spheres. *Powder Technology, 116*(1), 23–32. https://doi.org/10.1016/S0032-5910(00)00356-9. https://www.sciencedirect.com/science/article/pii/S0032591000003569

Zhao, B., An, X., Wang, Y., Qian, Q., Yang, X., & Sun, X. (2017). Dem dynamic simulation of tetrahedral particle packing under 3d mechanical vibration. *Powder Technology, 317*, 171–180. https://doi.org/10.1016/j.powtec.2017.04.048. https://www.sciencedirect.com/science/article/pii/S0032591017303455. URL.

Zhao, B., An, X., Wang, Y., Zhao, H., Shen, L., Sun, X., & Zou, R. (2020). Packing of different shaped tetrahedral particles: Dem simulation and experimental study. *Powder Technology, 360*, 21–32. https://doi.org/10.1016/j.powtec.2019.09.072. https://www.sciencedirect.com/science/article/pii/S0032591019307971

Zhao, B., An, X., Zhao, H., Gou, D., Shen, L., & Sun, X. (2020). Dem simulation on random packings of binary tetrahedron-sphere mixtures. *Powder Technology, 361*, 160–170. https://doi.org/10.1016/j.powtec.2019.09.055. https://www.sciencedirect.com/science/article/pii/S0032591019307788

Zhou, J., Zhang, Y., & Chen, J. K. (2009). Numerical simulation of random packing of spherical particles for powder-based additive manufacturing. *Journal of Manufacturing Science and Engineering, 131*(3), Article 031004. https://doi.org/10.1115/1.3123324. arXiv: https://asmedigitalcollection.asme.org/manufacturingscience/article-pdf/131/3/031004/5936649/031004_1.pdf.